

LEVERAGING ENSEMBLE-BASED SEMI-SUPERVISED LEARNING FOR ILLICIT ACCOUNT DETECTION IN ETHEREUM DEFI TRANSACTIONS

Shabnam Fazlani*

Department of Electrical Engineering
Sharif University of Technology
Tehran, Iran
shabnam.fazlani@ee.sharif.edu

Mohammad Mowlavi Sorond*

Department of Computer Engineering
Sharif University of Technology
Tehran, Iran
mohammad.molavi21@sharif.edu

Arsalan Masoudifard*

Department of Computer Engineering
Sharif University of Technology
Tehran, Iran
arsalan.masoudi@sharif.edu

Shaghayegh Fazlani

Department of Mathematics
Stanford University
Stanford, CA, USA
fazlani@stanford.edu

ABSTRACT

The advent of smart contracts has enabled the rapid rise of Decentralized Finance (DeFi) on the Ethereum blockchain, offering substantial rewards in financial innovation and inclusivity. This growth, however, is accompanied by significant security risks such as illicit accounts engaged in fraud. Effective detection is further limited by the scarcity of labeled data and the evolving tactics of malicious accounts. To address these challenges with a robust solution for safeguarding the DeFi ecosystem, we propose **SLEID**, a Self-Learning Ensemble-based Illicit account Detection framework. SLEID uses an Isolation Forest model for initial outlier detection and a self-training mechanism to iteratively generate pseudo-labels for unlabeled accounts, enhancing detection accuracy. Experiments on 6,903,860 Ethereum transactions with extensive DeFi interaction coverage demonstrate that SLEID significantly outperforms supervised and semi-supervised baselines with **+2.56** percentage-point precision, comparable recall, and **+0.90** percentage-point F1—particularly for the minority illicit class—alongside **+3.74** percentage-points higher accuracy and improvements in PR-AUC, while substantially reducing reliance on labeled data.

1 INTRODUCTION

Ethereum’s rapid growth as a smart-contract platform, especially through Decentralized Finance (DeFi), has expanded both innovation and attack surfaces. Its open, permissionless design reduces centralized oversight and enables adversaries to exploit protocol and ecosystem vulnerabilities (Qin et al., 2021; Schär, 2021; Zhou et al., 2023). The U.S. Treasury’s 2023 DeFi Risk Assessment highlights non-compliance with AML/CFT by many services and the resulting appeal to illicit actors; as of December 2022, over 2,000 DeFi services collectively held \$39.77B in TVL, with \$15.85B in decentralized exchanges (U.S. Department of the Treasury, 2023). Despite declines in overall illicit flows (from \$31.5B to \$22.2B) and mixer inflows, tactics shifted toward DeFi-centric rails: centralized exchanges remained the main off-ramps, and cross-chain bridges received \$743.8M from illicit addresses, underscoring DeFi’s growing role in laundering pathways (Chainalysis, 2024).

Detecting malicious accounts on Ethereum is essential. These accounts are often used to launder funds through exchanges, mixers, and lending platforms, taking advantage of pseudonymity to hide where the money comes from (Fu et al., 2023a). Phishing scams also target users and damage trust in

*These authors contributed equally to this work.

the ecosystem, making the accurate detection and mitigation of illicit accounts even more important (Wu et al., 2020).

Prior approaches to illicit account detection include:

- **Supervised learning:** classifiers (e.g., XGBoost) trained on labeled transaction histories to identify suspicious accounts (Farrugia et al., 2020; Palaiokrassas et al., 2023).
- **Unsupervised/rule-based methods:** risk-rating via suspiciousness, reliability, and trustiness metrics with network propagation for flexible fraud detection beyond binary labels (Fu et al., 2023b).
- **Visual analysis and anomaly detection:** multi-view interfaces combining LOF and DBSCAN to surface both high-frequency and low-profile patterns for human-in-the-loop investigation (Zhou et al., 2024).

However, these methods have limitations. Supervised models rely on scarce labeled data, limiting generalizability to evolving illicit activity. Risk-rating frameworks use subjective thresholds and struggle to scale on large transaction networks, causing inconsistent performance (Moradipari et al., 2022; Lee et al., 2023). Visual analysis improves interpretability but demands extensive manual validation and is prone to human error.

To address these challenges, we propose an ensemble semi-supervised framework for identifying illicit addresses within a batch of accounts (Figure 1). We first expand the batch and build a feature-rich dataset. We then use Isolation Forest for outlier detection, following Ripan et al. (2021), to filter outliers and select high-confidence normal accounts for more reliable supervised learning. Next, the supervised ensemble is trained iteratively with self-training: it generates pseudo-labels for the remaining unlabeled data and incorporates high-confidence predictions back into the training set. This reduces reliance on labeled data and enables learning from nuanced behaviors present in the unlabeled accounts.

Contributions.

- **Selective Dataset Acquisition.** We expand seeds via network neighbors and apply feature-based filtering to build a *DeFi-rich* dataset. Prioritizing DeFi interactions matters because laundering, swaps, and lending create informative, complex patterns that strengthen downstream detection.
- **Reliable Pseudo-Labeling.** An Isolation Forest flags outliers and screens stable normal accounts, producing dependable pseudo-labels from unlabeled addresses and improving the quality of the training signal.
- **Self-Learning Supervised Ensemble.** An iterative self-training loop adds confident predictions back into the training set, progressively sharpening decision boundaries and improving minority-class (illicit) detection.
- **Label Efficiency.** The integrated pipeline achieves strong illicit-account detection while substantially reducing reliance on scarce labeled data, enabling scalable deployment on large transaction graphs.

The remainder of this paper is organized as follows. Section 2 reviews related work. Section 3 describes the dataset, feature extraction, and data preprocessing. Section 4 presents the semi-supervised ensemble framework. Section 5 details the experimental setup and evaluations. Section 6 discusses the results and insights on interpretability and self-learning. Section 7 concludes the paper with a summary of findings and potential future directions for research.

2 RELATED WORKS

Detecting illicit accounts in cryptocurrency networks has received significant attention, with many works focusing on money laundering due to its prevalence and connections to other blockchain attacks. In the following, we summarize representative approaches for illicit account detection and AML.

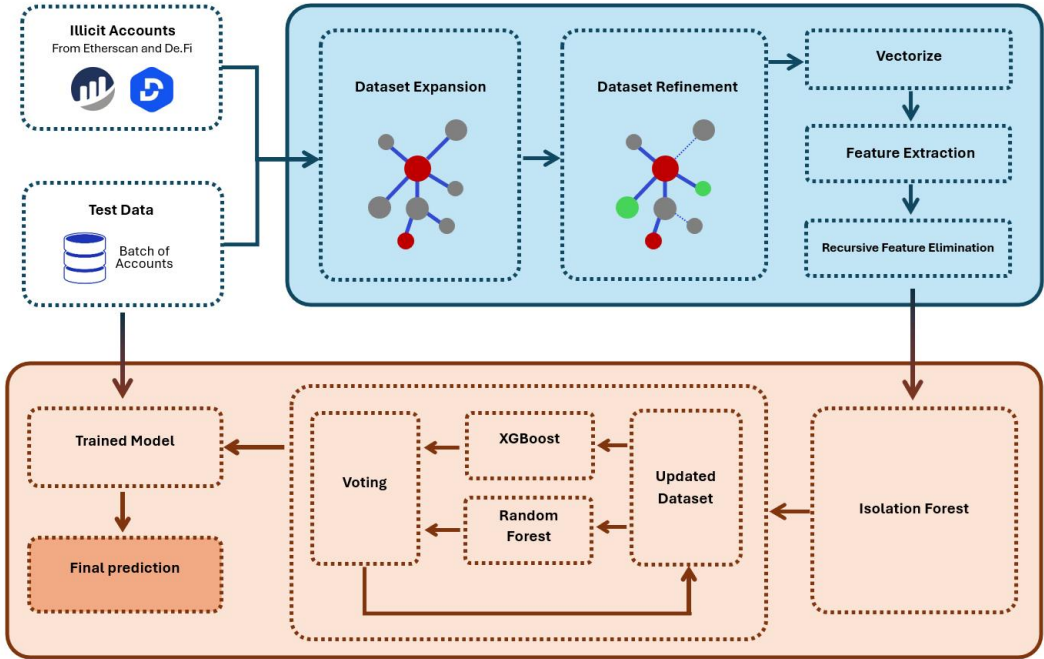


Figure 1: **Methodology overview for illicit account detection in the DeFi ecosystem.** The pipeline consists of three main components: dataset preparation, model training, and prediction. Illicit accounts are initially sourced from Etherscan and DeFi, followed by dataset expansion and refinement through network analysis. After vectorization and feature extraction, recursive feature elimination is applied to optimize the features. An isolation forest detects outliers, which are then used to update the dataset. The updated dataset is fed into a voting-based ensemble model combining XGBoost and Random Forest classifiers. The trained model is evaluated on a batch of test accounts to produce the final predictions on illicit activity.

Recent AML research introduces techniques to improve detection accuracy and reduce investigation costs (Abbasian et al., 2024; Rajabzadeh et al., 2024b). Labanca et al. (Labanca et al., 2022) propose an active learning framework that combines supervised and unsupervised methods with targeted selection strategies, outperforming existing AML systems. Jensen and Iosifidis (Jensen & Iosifidis, 2023) review statistical and machine learning approaches used in banks, emphasizing client risk profiling, challenges in flagging suspicious behavior, and the promise of deep learning and synthetic data. Wu et al. (Wu et al., 2024a) analyze Ethereum asset flows after cyber heists, using taint analysis to reveal laundering tactics such as token swaps and counterfeit token creation, highlighting practices that exceed traditional AML frameworks.

Graph-based techniques address AML in complex networks. Hyun et al. (Hyun et al., 2023) use a multi-relational GNN with adaptive neighbor sampling to handle sparse node features and class imbalance, improving detection. Cheng et al. (Cheng et al., 2023) model organized criminal behavior with a group-aware deep graph approach, capturing community patterns. Zhou et al. (Zhou et al., 2024) develop a visual analysis system that integrates anomaly detection to support supervisors in identifying laundering tactics. Together, these works underscore the effectiveness of graph learning for AML in financial networks.

Beyond AML, several studies target fraud detection in cryptocurrency networks. Umer et al. (Umer et al., 2023) propose a CNN–LSTM ensemble with bagging and boosting, achieving 96.4% accuracy on Ethereum transactions. Patel et al. (Vatsal Patel & Rajasegarar, 2020) introduce a graph-based anomaly framework using One-Class GNNs, outperforming non-graph baselines (Isolation Forest, One-Class SVM) by leveraging inter-node relationships relevant to smart contract and DAO-related anomalies.

Additional graph learning models further improve blockchain fraud detection. Kanezashi et al. (Kanezashi et al., 2018) show that heterogeneous RGCN surpasses homogeneous GNNs for phishing and illicit activity detection. Liu et al. (Liu et al., 2023) present GTN2vec, a graph embedding method using biased random walks and behavioral features (e.g., gas price, timestamps) to enhance money laundering detection. Sun et al. (Sun, 2024) propose ABGRL with adaptive attention to better represent low-degree nodes for phishing detection and Li et al. (Li et al., 2023) introduce SIEGE, a self-supervised incremental deep graph model that processes Ethereum data over time and improves phishing detection via combined spatial and temporal learning.

Moreover, Aziz et al. propose several ML/DL approaches for Ethereum fraud detection. They introduce an LGBM method for transactions with limited attributes, showing high accuracy and efficiency for gradient boosting (Aziz et al., 2022a;b). With Euclidean distance estimation, their LGBM outperforms Random Forest and XGBoost (up to 99.17%) (Aziz et al., 2022b). They further develop a deep model optimized with a hybrid Genetic Algorithm–Cuckoo Search, reaching 99.71% and surpassing random forest, logistic regression, and SVC (Aziz et al., 2023).

Non-graph anomaly detection has also been explored via semi-supervised learning and AI integration. Sanjalawe et al. (Sanjalawe & Al-E’mari, 2023) present ATD-SGAN, which generates synthetic data to improve IDS on Ethereum, boosting accuracy by 3.78%–11.05% and reducing false alarms to 0.15%. Olawale and Ebadinezhad (Olawale & Ebadinezhad, 2024) combine SVM and 1D CNNs for IoHT anomaly detection and use IPFS for secure, immutable storage. Poursaefai et al. (Poursaefai et al., 2020) employ traditional ML (Logistic Regression, SVM, Stacking, AdaBoost) for Ethereum, achieving an F1 of 0.996.

Graph-based techniques capture relational structure for anomaly detection (Rathore et al., 2025). Tan et al. (Tan et al., 2023) combine Node2Vec embeddings with a GCN classifier to detect suspicious accounts, attaining 96% accuracy. Rabieinejad et al. (Rabieinejad et al., 2021) propose a two-phase deep approach—DNN for attack detection, followed by K-means and supervised models (Decision Tree, Random Forest, Naive Bayes)—reaching 97.72% detection and 99.4% classification accuracy. Together, these graph-based models highlight the value of network structure analysis in enhancing anomaly detection capabilities in blockchain ecosystems.

3 DATASET CONSTRUCTION AND FEATURE ENGINEERING

3.1 DATASET COLLECTION AND CURATION

Our experiment aims to determine whether Ethereum account batches are illicit. We selected 581 anomalous accounts from a manually curated, externally corroborated set, linked to phishing schemes, rug pulls, heists, and flash loan attacks. Traditional time-frame-based collection methods face challenges as not all account transactions fall within chosen periods, and datasets remain highly imbalanced with illicit accounts comprising only 0.1% of totals, significantly hindering detection model performance. A more effective approach constructs a core set of known illicit accounts and expands through second-order neighboring accounts. This captures broader account interactions and provides comprehensive network views. By using known illicit accounts as cores and including their transaction partners, this method overcomes time-frame limitations by considering entire interaction networks, improving illicit activity identification reliability (Liu et al., 2023). Fu et al. (Fu et al., 2023b) implemented rule-based scoring evaluating three metrics: anonymity (identity concealment through limited transactions per account), wash trading (repetitive transactions artificially boosting volumes), and lifespan (duration between first/last transactions, with shorter spans indicating potential fraud). While high-risk accounts generated false positives, low-risk accounts proved reliably normal. We classified accounts scoring less than 0.2 across all criteria as normal accounts, effectively minimizing misclassification risk while maintaining stringent detection mechanisms.

Based on prior work (Wu et al., 2024b), fraudulent accounts involved in money laundering eventually transact with DeFi platforms for token swapping or lending. Research has shown (Palaiokrassas et al., 2023; Fazliani et al., 2025) that incorporating DeFi features significantly enhances ML model performance. Therefore, we prioritize accounts with higher DeFi transaction volumes, adding them to our core addresses for more informative complex interaction insights into both normal and fraudulent behavior.

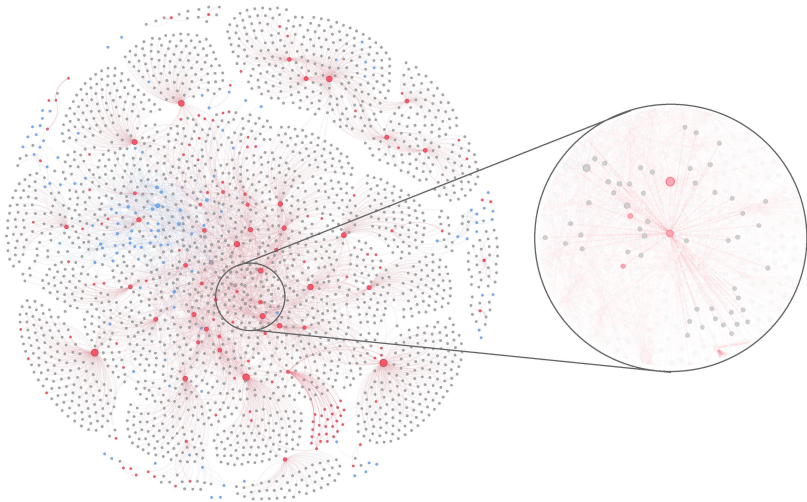


Figure 2: Network visualization of account interconnections. Blue, red, and gray nodes represent legitimate, illicit, and unknown accounts, respectively.

Our dataset expansion algorithm (detailed in Appendix A.1.1 Algorithm 1) iteratively adds addresses until illicit account ratios drop below 0.01. Starting with initialized address datasets and illicit ratios, it acquires new address layers, evaluating each one. Addresses are added if the risk scores fall below 0.2 or involve DeFi transactions. The process continues until the desired ratios are reached. The final dataset comprises 44,675 core addresses with all transactions investigated, totaling 1,888,553 accounts. Our core addresses with 1% illicit accounts are more informative and enable unsupervised methods to pseudo-label additional illicit accounts due to richer patterns. Data was collected from August 7th, 2015 until April 4, 2024.

Figure 2 shows illicit accounts that form clusters with interconnections at distances of only one node, often associated with collaborative phishing activities. Many gray nodes (unknown status) are embedded within illicit clusters, suggesting a high likelihood of suspicious behavior, which warrants further investigation. This interconnectedness underscores the need to analyze both known illicit accounts and neighbors to uncover hidden patterns of criminal behavior.

3.2 MODELING & PREPROCESSING

To effectively analyze the Ethereum ecosystem, we adopt directed graph representations. After exploring various graph models (Wu et al., 2021; Fazlani, 2024) including transaction graphs, address graphs, cluster graphs, and bipartite graphs (detailed comparison in Appendix), the **bipartite graph** emerged as optimal for our needs. With nodes divided into two distinct groups—users and transactions—bipartite graphs excel in depicting interactions without overlap, maintaining clear distinction between participants and their transactions (Geng et al., 2021).

The bipartite graph structure (illustrated in Appendix A.1.2 Figure 4) distinctively associates each user account with their transactions, simplifying detection of anomalous patterns such as unusually high transaction volumes within short timeframes. This explicit demarcation between user and transaction nodes significantly improves irregular behavior identification, facilitates recognition of habitual user behaviors, and enables the extraction of sophisticated features like node centrality and transaction clustering essential for robust anomaly detection models.

The raw dataset was preprocessed to handle missing and extreme values. Non-informative features (tag, address, type) were removed. Missing values were imputed with means, and infinite values were replaced with NaN before dropping. The 99th percentile of each feature served as upper bounds to clip extreme outliers, minimizing noise impact and improving model stability.

3.3 FEATURE EXTRACTION

We employ diverse features capturing blockchain interaction characteristics:

- **Graph-Related Features:** Basic metrics (in-degree, out-degree, centrality) identifying central nodes and suspicious activity hubs.
- **Temporal Features:** Transaction frequency, timing, and recipient diversity monitoring behavioral consistency and detecting irregular patterns.
- **Node Features:** Account-specific attributes (balance, creation date, smart contract participation) providing stability and history insights.
- **Transaction Features:** Specific characteristics (average value, fees, timestamps, execution order) understanding flows and norm deviations.
- **Volatility Indicators:** Sudden changes in volumes, fees, or frequency detecting manipulation or fraud, particularly flash anomalies affecting market stability.
- **Neighborhood Features:** Aggregated neighboring node data identifying local subnetwork characteristics influencing node behavior, including average transaction size, frequency, and fee structures within immediate network vicinity.

This comprehensive feature integration enables robust detection of anomalous behaviors deviating from typical Ethereum DeFi transaction patterns, enhancing detection accuracy while providing detailed network dynamics perspective essential for risk mitigation in the rapidly evolving Ethereum landscape. A complete list of features and definitions is provided in Appendix A.1.4.

4 METHODOLOGY

4.1 OVERVIEW

We tackle the large pool of unknown labels by combining anomaly detection with semi-supervised learning. After vectorization and feature extraction (with recursive feature elimination; see Appx. A.1.3), we apply an Isolation Forest to the unknown subset to surface likely illicit addresses. These predictions are used as pseudo-labels to augment the labeled set, after which a supervised ensemble is trained, iteratively refined with self-learning, and evaluated. The full pipeline is shown in Figure 1.

4.2 LABEL ASSIGNMENT

We run Isolation Forest on the unknown class (contamination = 0.5%). Its predictions partition unknowns into (i) *filtered unknown* (non-outliers) and (ii) *illicit candidates* (outliers). Illicit candidates are added to the labeled set as pseudo-labeled illicit samples, expanding the variety of illicit examples and helping mitigate class imbalance. The filtered-unknown pool is retained for the subsequent self-learning stage.

4.3 ENSEMBLE TRAINING AND CROSS-VALIDATION

We construct a supervised ensemble over **Random Forest (RF)** and **XGBoost (XGB)** using *soft voting*, i.e., averaging class probabilities with equal weights to produce the final prediction. Hyperparameters for both models are tuned with Optuna to maximize cross-validated F1 on the augmented labeled set.

Random Forest (RF). The Optuna search covers the number of trees (estimators), maximum depth, minimum samples required to split an internal node, and *class weights* to address imbalance. Each candidate configuration is evaluated via stratified cross-validation and scored by the mean F1.

XGBoost (XGB). The search varies maximum depth, learning rate, number of boosting rounds (estimators), and regularization terms to control overfitting. As with RF, candidates are scored by cross-validated F1.

Evaluation protocol. We use **5-fold stratified** cross-validation. In each fold, RF and XGB are trained on the training split of the augmented labeled data; their class-probability outputs are averaged for ensemble predictions on the validation split. We record precision, recall, F1, and accuracy for both licit and illicit classes and report the aggregated results across folds. Full model settings, search spaces, and cross-validation configuration are provided in Appx. A.1.6.

4.4 SELF-LEARNING ITERATIVE APPROACH

In addition to cross-validation, an iterative self-learning process was incorporated to further improve classification performance. After each fold, the trained Voting Classifier was applied to the filtered unknown data. The model’s predicted probabilities for the unknown samples were used to identify the most confident predictions, based on a confidence threshold (e.g., 90%).

During each iteration:

- Confident predictions were added to the training dataset.
- The classifier was retrained on the expanded dataset (including the confident pseudo-labeled samples).
- The process continued for a fixed number of iterations (e.g., 5) or until no confident samples remained.

This pseudo-labeling strategy enabled continuous learning from both labeled and pseudo-labeled data, improving generalization and robustness, particularly for the minority illicit class.

The final model after each fold was evaluated on validation data, retaining the iteration yielding best recall for the illicit class. For each cross-validation fold, optimal performance metrics—recall, precision, F1-score, and accuracy—were recorded for both classes, providing comprehensive evaluation with emphasis on illicit class recall due to anomaly detection importance. The integration of hyperparameter optimization, ensemble learning, and self-learning pseudo-labeling effectively improved model performance in distinguishing licit and illicit activities despite substantial class imbalance.

5 EXPERIMENTS AND RESULTS

5.1 MODEL PERFORMANCE COMPARISON

We introduce our model, the **Self-Learning Ensemble-based Illicit account Detection (SLEID)** system. To evaluate SLEID’s effectiveness, we conducted comprehensive comparison with six other models: two traditional supervised learning algorithms—XGBoost and Random Forest—and four semi-supervised methods including IF-One-Class-SVM, IF-LOF, and Isolation Forests integrated with supervised classifiers (IF-XGBoost and IF-RF). The performance of each model was assessed using key metrics such as precision, recall, and F1-score for both licit and illicit classes, along with the overall accuracy.

Table 1 presents the performance comparison between different models for detecting illicit accounts. As seen from the table, the SLEID outperforms other models in terms of Recall, F1-score, and Accuracy, achieving the highest Recall at 95.78%, F1-score at 96.80%, and Accuracy at 99.44%. The IF-RF model shows the highest Precision at 99.04%, but SLEID offers a more balanced performance across all metrics, making it the most effective model for detecting illicit accounts in this scenario.

As depicted in Figure 3, SLEID achieves higher precision, recall, and F1-score for the illicit class, indicating its effectiveness in identifying suspicious activities within the Ethereum network. On the other hand, when evaluating the licit class, all models exhibit similar performance, with minor variations.

5.2 COMPARISON WITH PREVIOUS WORKS

In this section, we compare our proposed SLEID framework with prior studies on detecting illicit activities in the Ethereum ecosystem. Both methodological innovations and empirical results are highlighted to underscore the contributions and effectiveness of our approach. Note that our results

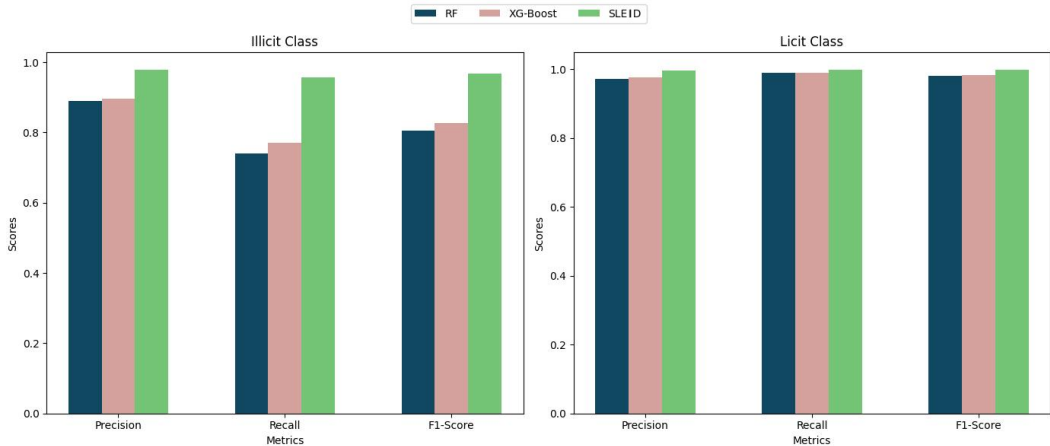


Figure 3: Performance Comparison of Illicit and Licit Class Detection Across Different Models

Model	Precision	Recall	F1	Accuracy
XG-Boost	89.53	76.96	82.68	96.79
Random-Forest	88.97	74.10	80.57	96.47
IF-One-Class-SVM	56.81	92.64	70.39	82.53
IF-LOF	70.66	85.17	77.20	88.67
IF-XGBoost	98.43	93.96	96.13	99.34
IF-RF	99.04	94.12	96.51	99.40
SLEID	97.86	95.78	96.80	99.44

Table 1: Comparison of models' performance on finding illicit accounts

are based on a unique dataset specifically tailored to our study, and direct comparisons with other works may not be entirely conclusive due to differences in datasets and evaluation settings.

5.2.1 METHODOLOGY COMPARISON

Our framework introduces a novel ensemble-based semi-supervised learning approach for detecting illicit accounts. The key methodological components are:

- **Reduced Label Dependence:** Unlike Farrugia et al. (Farrugia et al., 2020) and Palaiokrasas et al. (Palaiokrasas et al., 2023), which rely heavily on labeled datasets, SLEID leverages pseudo-labeling through an Isolation Forest to iteratively incorporate unlabeled data, significantly reducing dependence on labeled data.
- **Ensemble Architecture:** Combining XGBoost and Random Forest classifiers, SLEID ensures balanced performance across multiple evaluation metrics. This approach outperforms single-model frameworks like GTN2vec (Liu et al. (Liu et al., 2023)) and SIEGE (Li et al. (Li et al., 2023)), which focus on specialized tasks like money laundering or phishing.
- **Iterative Self-Learning:** SLEID incorporates high-confidence predictions iteratively, refining the pseudo-labels and adapting to the data over multiple iterations. This mechanism is particularly effective for improving recall, a metric critical for fraud detection.

5.2.2 RESULTS COMPARISON

The empirical performance of SLEID demonstrates superiority across multiple metrics. Because our dataset was curated specifically for this study—differing from prior corpora in scope, time span, and labeling protocol—cross-paper comparisons should be viewed as *indicative* rather than strictly conclusive.

Metric	SLEID (Our Work)	Liu et al. (Liu et al., 2023)	Son et al. (Son et al., 2024)
Accuracy	99.44%	95.7%	96.5%
Precision	97.86%	95.3%	96.5%
Recall	95.78%	96.4%	96.3%
F1-Score	96.80%	95.9%	96.4%

Table 2: Comparison of Results with Previous Work

5.2.3 KEY TAKEAWAYS

SLEID results are dataset-specific and may not directly compare to other works focusing on specific illicit activity subsets. SLEID achieved remarkable 99.44% accuracy, surpassing Farrugia et al.’s 96.3% (Farrugia et al., 2020) and GTN2vec’s 95.7% (Liu et al., 2023), with iterative self-learning contributing significantly. The framework effectively balances precision (97.86%) and recall (95.78%), contrasting prior methods that prioritize one over the other or focus on specific fraud subsets. With 96.80% F1-score, SLEID excels at balancing precision/recall for diverse fraud patterns, unlike specialized methods such as SIEGE (Li et al., 2023). Similarly, Son et al. (Son et al., 2024) proposed a semi-supervised DAE-MLP for anomaly detection in blockchain-based supply chains, achieving 96.5% accuracy, 96.5% precision, and 96.3% recall.

In addition, Ouyang et al. (Ouyang et al., 2024) introduced Bit-CHetG, a subgraph-based heterogeneous GNN framework enhanced with supervised contrastive learning for Bitcoin money laundering detection. Evaluated on the Elliptic and BlockSec datasets, Bit-CHetG achieved strong empirical results, reporting Micro-Precision of 90.5%, Micro-Recall of 89.3%, and Micro-F1 of 91.9% on the Elliptic dataset, representing at least a 5% improvement over state-of-the-art baselines such as Sub-GNN, Tsgn, HAN, and MAGNN. These results underscore the advantage of incorporating subgraph contrastive learning and heterogeneous graph modeling in capturing illicit group behaviors.

SLEID outperforms through methodological advancements including reduced label dependence, ensemble architecture, and iterative self-learning. However, dataset-specific results warrant caution in direct comparisons. Future studies should standardize datasets and evaluation protocols for comprehensive benchmarking.

6 DISCUSSION

Our results demonstrate consistent performance in detecting licit accounts across different architectures, indicating that the learned representations effectively capture legitimate blockchain transaction patterns. This consistency suggests that our feature engineering and model training successfully identify the diverse characteristics of legitimate activities, ranging from standard transfers to complex DeFi interactions. The robust performance across XGBoost, Random Forest, and SLEID architectures validates the quality of our feature extraction and preprocessing pipeline for distinguishing legitimate behavior patterns.

The self-learning process reveals an interesting phenomenon where performance gains diminish after the third iteration (See Appendix A.2.1). This occurs as noise accumulates in pseudo-labeled data and the model extracts most valuable information from unlabeled samples early in the process. Beyond this point, additional iterations contribute minimally while risking overfitting. Optimal strategies include terminating self-learning after three iterations or implementing sophisticated filtering mechanisms with confidence thresholds and ensemble weighting to maintain data quality.

While ensemble models traditionally face interpretability challenges as “black box” systems, we addressed this by conducting SHAP- and LIME-based analyses (Appendix A.2.2) to surface feature contributions and decision logic. In addition, we explicitly account for class imbalance and false-positive risk by reporting minority-class PR-AUC, class-weighted F1, and MCC; we also audit the ranked false positive cohort with feature attributions for practitioner review (Appendix A.2.5, A.2.4).

7 CONCLUSION AND FUTURE WORKS

7.1 CONCLUSION

In this paper, we propose SLEID, a novel ensemble-based semi-supervised learning framework designed to detect illicit accounts in Ethereum’s Decentralized Finance (DeFi) transactions. By utilizing an Isolation Forest for outlier detection and a self-training mechanism for pseudo-labeling, our method addresses key challenges including the scarcity of labeled data and the complex, evolving tactics employed by malicious actors. The experimental results show that SLEID outperforms traditional supervised models, achieving high precision, recall, and F1-scores, particularly in the detection of illicit accounts. These findings highlight the effectiveness of semi-supervised techniques in enhancing the security of blockchain ecosystems, providing a scalable and adaptable solution for real-world financial networks, such as Ethereum. Ultimately, our approach contributes to the broader efforts to improve security and trust within DeFi ecosystems, where the identification and mitigation of fraudulent activities remains critical.

7.2 FUTURE WORKS

While our proposed SLEID model demonstrates high efficacy in detecting illicit accounts, there are several avenues for further research to enhance its capabilities:

1. **Integration of More Complex Graph Features:** Future work could explore the inclusion of more advanced graph-based features, such as multi-hop relationships and temporal patterns in transaction flows, to improve the model’s ability to detect subtle illicit activities.
2. **Real-time Detection:** Expanding SLEID to operate in a real-time or near-real-time environment would enable faster identification and prevention of fraudulent transactions as they occur, increasing the practical utility of the model for financial institutions.
3. **Cross-chain Analysis:** With the rise of multi-chain ecosystems, investigating how SLEID can be extended to detect illicit accounts across different blockchain networks, beyond Ethereum, could significantly expand its applicability.
4. **Further Refinement of Self-learning Techniques:** Although the self-learning mechanism in SLEID proved effective, experimenting with different confidence thresholds and more sophisticated pseudo-labeling methods could further enhance model robustness, particularly in handling class imbalance and reducing false positives.

ACKNOWLEDGMENTS

We would like to express our sincere gratitude to Prof. Mohammad Ali Maddah-Ali for his invaluable guidance and insightful suggestions that significantly enhanced the quality of this work.

REFERENCES

Mahyar Abbasian, Taha Rajabzadeh, Ahmadreza Moradipari, Seyed Amir Hossein Aqajari, Hongsheng Lu, and Amir M Rahmani. Controlling the latent space of gans through reinforcement learning: A case study on task-based image-to-image translation. In *Proceedings of the 39th ACM/SIGAPP Symposium on Applied Computing*, pp. 1061–1063, 2024.

Rabia Musheer Aziz, Mohammed Farhan Baluch, Sarthak Patel, and Abdul Hamid Ganie. Lgbm: a machine learning approach for ethereum fraud detection. *International Journal of Information Technology*, 14(7):3321–3331, 2022a.

Rabia Musheer Aziz, Mohammed Farhan Baluch, Sarthak Patel, and Pavan Kumar. A machine learning based approach to detect the ethereum fraud transactions with limited attributes. *Karbala International Journal of Modern Science*, 8(2):139–151, 2022b.

Rabia Musheer Aziz, Rajul Mahto, Kartik Goel, Aryan Das, Pavan Kumar, and Akash Saxena. Modified genetic algorithm with deep learning for fraud transactions of ethereum smart contract. *Applied Sciences*, 13(2):697, 2023.

Chainalysis. Money laundering activity spread across more service deposit addresses in 2023, plus new tactics from lazarus group. <https://www.chainalysis.com/blog/2024-crypto-money-laundering/>, February 2024.

Dawei Cheng, Yujia Ye, Sheng Xiang, Zhenwei Ma, Ying Zhang, and Changjun Jiang. Anti-money laundering by group-aware deep graph learning. *IEEE Trans. on Knowledge and Data Engineering*, 35(12):12444–12456, 2023.

Simone Farrugia et al. Detection of illicit accounts over the ethereum blockchain. *Expert Systems with Applications*, pp. 113318, 2020. doi: 10.1016/j.eswa.2020.113318.

Shaghayegh Fazlani. Hausdorff measure bound for the nodal sets of neumann laplace eigenfunctions, 2024. URL <https://arxiv.org/abs/2311.09686>.

Shaghayegh Fazlani, Zachary Frangella, and Madeleine Udell. Enhancing physics-informed neural networks through feature engineering, 2025. URL <https://arxiv.org/abs/2502.07209>.

Qishuang Fu, Dan Lin, Yiyue Cao, and Jiajing Wu. Does money laundering on ethereum have traditional traits? *Electronics*, 12(14):3180, 2023a. doi: 10.3390/electronics12143180.

Qishuang Fu, Dan Lin, Jiajing Wu, and Zibin Zheng. A general framework for account risk rating on ethereum: toward safer blockchain technology. *IEEE Transactions on Computational Social Systems*, 11(2):1865–1875, 2023b.

Jinke Geng, Yi Li, Li Fang, and Ping Chen. Vw-dbg: A dynamically evolving bitcoin transaction network model. *IEEE Transactions on Network Science and Engineering*, 9(2):356–363, 2021.

Woochang Hyun, Jaehong Lee, and Bongwon Suh. Anti-money laundering in cryptocurrency via multi-relational graph neural network. In *PAKDD, LNAI 13936*, pp. 118–130, 2023.

Rasmus Ingemann Tuffveson Jensen and Alexandros Iosifidis. Fighting money laundering with statistics and machine learning. *IEEE Access*, 11:8889–8902, 2023.

Hiroki Kanezashi, Toyotaro Suzumura, Xin Liu, and Takahiro Hirofuchi. Ethereum fraud detection with heterogeneous graph neural networks. In *Conference Proceedings*, 2018.

D. Labanca, L. Primerano, M. Markland-Montgomery, M. Polino, M. Carminati, and S. Zanero. Amaretto: An active learning framework for money laundering detection. *IEEE Access*, 10: 41720–41732, 2022.

Nathan RA Lee, Yudan Guo, Agnetta Y Cleland, E Alex Wollack, Rachel G Gruenke, Takuma Makihara, Zhaoyou Wang, Taha Rajabzadeh, Wentao Jiang, Felix M Mayor, et al. Strong dispersive coupling between a mechanical resonator and a fluxonium superconducting qubit. *PRX Quantum*, 4(4):040342, 2023.

Shuo Li et al. Siege: Self-supervised incremental deep graph learning for ethereum phishing scam detection. 2023. doi: 10.1145/3581783.3612461.

Jiayi Liu, Changchun Yin, Hao Wang, Xiaofei Wu, Dongwan Lan, Lu Zhou, and Chunpeng Ge. Graph embedding-based money laundering detection for ethereum. *Electronics*, 12(14):3180, 2023. doi: 10.3390/electronics12143180.

Arsalan Masoudifard, Mohammad Mowlavi Sorond, Moein Madadi, Mohammad Sabokrou, and Elahe Habibi. Leveraging graph-rag and prompt engineering to enhance llm-based automated requirement traceability and compliance checks. *arXiv preprint arXiv:2412.08593*, 2024.

Ahmadreza Moradipari, Mohammad Ghavamzadeh, Taha Rajabzadeh, Christos Thrampoulidis, and Mahnoosh Alizadeh. Multi-environment meta-learning in stochastic linear bandits. In *2022 IEEE International Symposium on Information Theory (ISIT)*, pp. 1659–1664. IEEE, 2022.

Oluwaseun Priscilla Olawale and Sahar Ebadinezhad. Cybersecurity anomaly detection: Ai and ethereum blockchain for a secure and tamperproof ioht data management. *IEEE Access*, 2024.

Shiyu Ouyang, Qianlan Bai, Hui Feng, and Bo Hu. Bitcoin money laundering detection via subgraph contrastive learning. *Entropy*, 26(3):211, 2024.

Georgios Palaiokrassas et al. Leveraging machine learning for multichain defi fraud detection. *ArXiv.org*, 2023. Available at: <https://arxiv.org/abs/2306.07972>.

Farimah Poursafaei, Ghaith Bany Hamad, and Zeljko Zilic. Detecting malicious ethereum entities via application of machine learning classification. In *2020 2nd conference on blockchain research & applications for innovative networks and services (BRAINS)*, pp. 120–127. IEEE, 2020.

Kaihua Qin, Liyi Zhou, Pablo Gau, Peter Jovanovic, and Arthur Gervais. An empirical study of defi liquidations: Incentives, risks, and instabilities. In *Proceedings of the 2021 ACM Conference on Economics and Computation*, pp. 1–18, 2021. doi: 10.1145/3487552.3487811.

Elnaz Rabieinejad, Abbas Yazdinejad, and Reza M Parizi. A deep learning model for threat hunting in ethereum blockchain. In *2021 IEEE 20th International Conference on Trust, Security and Privacy in Computing and Communications (TrustCom)*, pp. 1185–1190. IEEE, 2021.

Taha Rajabzadeh, Mohammad Hosein Mousavi, Sajjad Abdollahramezani, Mohammad Vahid Jamali, and Jawad A Salehi. Femtosecond cdma using dielectric metasurfaces: Design procedure and challenges. *arXiv preprint arXiv:1712.00834*, 2017.

Taha Rajabzadeh, Christopher J Sarabalis, Okan Atalar, and Amir H Safavi-Naeini. Photonics-to-free-space interface in lithium niobate-on-sapphire. In *CLEO: Science and Innovations*, pp. STu4J–6. Optica Publishing Group, 2020.

Taha Rajabzadeh, Zhaoyou Wang, Nathan Lee, Takuma Makihara, Yudan Guo, and Amir H Safavi-Naeini. Analysis of arbitrary superconducting quantum circuits accompanied by a python package: Sqcircuit. *Quantum*, 7:1118, 2023.

Taha Rajabzadeh, Alex Boulton-McKeehan, Sam Bonkowsky, David I Schuster, and Amir H Safavi-Naeini. A general framework for gradient-based optimization of superconducting quantum circuits using qubit discovery as a case study. *arXiv preprint arXiv:2408.12704*, 2024a.

Taha Rajabzadeh, Alexander Boulton-McKeehan, Sam Bonkowsky, and Amir Safavi-Naeini. Gradient-based optimization of superconducting quantum circuit designs-part 2. In *APS March Meeting Abstracts*, volume 2024, pp. A47–010, 2024b.

Pratik Rathore, Zachary Frangella, Sachin Garg, Shaghayegh Fazlani, Michał Dereziński, and Madeleine Udell. Turbocharging gaussian process inference with approximate sketch-and-project, 2025. URL <https://arxiv.org/abs/2505.13723>.

Rony Chowdhury Ripan, Iqbal H. Sarker, Md Musfiq Anwar, Md. Hasan Furhad, Fazle Rahat, Mohammed Moshiul Hoque, and Muhammad Sarfraz. An isolation forest learning based outlier detection approach for effectively classifying cyber anomalies. In *2021 International Conference on Data Science and Security (ICDSS)*, 2021. doi: 10.1007/springer-12345.

Yousef K Sanjalawe and Salam R Al-E'mari. Abnormal transactions detection in the ethereum network using semi-supervised generative adversarial networks. *IEEE Access*, 2023.

Fabian Schär. Decentralized finance: On blockchain- and smart contract-based financial markets. *Papers.ssrn.com*, 2021. Available at: https://papers.ssrn.com/sol3/papers.cfm?abstract_id=3843844.

Do Hai Son, Bui Duc Manh, Tran Viet Khoa, Nguyen Linh Trung, Dinh Thai Hoang, Hoang Trong Minh, Yibeltal Alem, and Le Quang Minh. Semi-supervised learning for anomaly detection in blockchain-based supply chains. In *2024 23rd International Symposium on Communications and Information Technologies (ISCIT)*, pp. 140–145. IEEE, 2024.

Haojie Sun. Adaptive attention-based graph representation learning to detect phishing accounts on the ethereum blockchain. *IEEE Transactions on Network Science and Engineering*, pp. –, 2024. doi: 10.1109/TNSE.2024.3355089.

Runnan Tan, Qingfeng Tan, Qin Zhang, Peng Zhang, Yushun Xie, and Zhao Li. Ethereum fraud behavior detection based on graph neural networks. *Computing*, 105(10):2143–2170, 2023.

Qasim Umer, Jian-Wei Li, Muhammad Rehan Ashraf, Rab Nawaz Bashir, and Hamid Ghous. Ensemble deep learning based prediction of fraudulent cryptocurrency transactions. *IEEE Access*, 2023.

U.S. Department of the Treasury. Defi illicit finance risk assessment, 2023. Available at: <https://home.treasury.gov/news/press-releases/jy1391>.

Lei Pan Vatsal Patel and Sutharshan Rajasegarar. Graph deep learning based anomaly detection in ethereum blockchain network. In *International Conference on Network and System Security (NSS)*, pp. 132–148. Springer, 2020. doi: 10.1007/978-3-030-65745-1_8.

Jiajing Wu, Qi Yuan, Dan Lin, Weijia You, Wei Chen, Chen Chen, and Zibin Zheng. Who are the phishers? phishing scam detection on ethereum via network embedding. *IEEE Transactions on Systems, Man, and Cybernetics: Systems*, 52(2):1156–1166, 2020. doi: 10.1109/TSMC.2020.2979892.

Jiajing Wu, Jie Liu, Yijing Zhao, and Zibin Zheng. Analysis of cryptocurrency transactions from a network perspective: An overview. *Journal of Network and Computer Applications*, 190:103139, 2021.

Jiajing Wu, Dan Lin, Qishuang Fu, Shuo Yang, Ting Chen, Zibin Zheng, and Bowen Song. Toward understanding asset flows in crypto money laundering through the lenses of ethereum heists. *IEEE Trans. on Information Forensics and Security*, 19:1994–2005, 2024a.

Jiawei Wu, Dongze Lin, Qian Fu, Sheng Yang, Tong Chen, Zibin Zheng, and Bo Song. Toward understanding asset flows in crypto money laundering through the lenses of ethereum heists. *IEEE Transactions on Information Forensics and Security*, 19:1994–2007, 2024b. doi: 10.1109/TIFS.2023.3346276.

Fangfang Zhou, Yunpeng Chen, Chunyao Zhu, Lijia Jiang, Xincheng Liao, Zengsheng Zhong, Xiaohui Chen, Yi Chen, and Ying Zhao. Visual analysis of money laundering in cryptocurrency exchange. *IEEE Trans. on Computational Social Systems*, 11(1):731–742, 2024.

Liyi Zhou, Xihan Xiong, Jens Ernstberger, Stefanos Chaliasos, Zhipeng Wang, Ye Wang, Kaihua Qin, Roger Wattenhofer, Dawn Song, and Arthur Gervais. Sok: Decentralized finance (defi) attacks. pp. 2444–2461, 2023.

A APPENDIX

A.1 EXPERIMENT SET UP

A.1.1 DATASET

The algorithm presented is used for expanding a dataset of addresses by iteratively adding new addresses until the ratio of illicit accounts in the dataset drops below a certain threshold (0.01 in this case). It starts by initializing an address dataset and calculating the current illicit account ratio. Then, it acquires new layers of addresses, evaluates each one, and adds it to the dataset if the risk score is below 0.2 or if the account is involved in DeFi transactions. After each iteration, the illicit ratio is updated, and the process continues until the desired ratio is met.

Algorithm 1 Dataset Expansion

```
1: initialize address_dataset
2: initialize illicit_ratio based on address_dataset
3: while illicit_ratio > 0.01 do
4:   Acquire the next layer of addresses and store it in temp_new_addresses
5:   for each address in temp_new_addresses do
6:     if risk_rate_score < 0.2 then
7:       add this address to address_dataset
8:     end if
9:     if is_DeFi_involved then
10:      add this address to address_dataset
11:    end if
12:  end for
13:  update illicit_ratio based on address_dataset
14: end while
```

A.1.2 MODELING

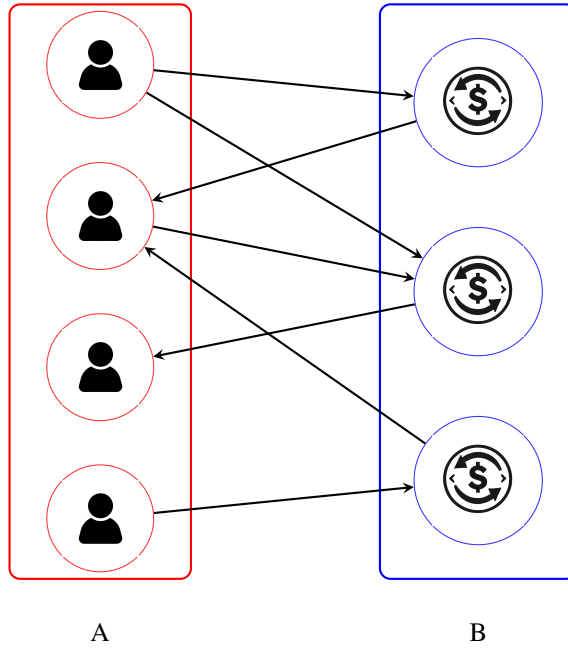
We explored various graph models to determine the most suitable representation for our dataset:

- **Transaction Graphs:** Nodes represent transactions, and directed edges reflect fund flows, incorporating attributes such as transaction timings, fees, amounts, and computational costs. These graphs are instrumental in identifying deviations in transaction patterns and costs.
- **Address Graphs:** These graphs feature addresses as nodes, with transactions between addresses forming the directed edges. By mapping address interactions, we enhance our ability to spot anomalous behaviors linked to specific addresses.
- **Cluster Graphs:** In these graphs, clusters of addresses serve as nodes. Directed edges between clusters help in detecting unusual transaction flows, thus highlighting potential anomalies in broader network behaviors.
- **Bipartite Graphs:** With nodes divided into two distinct groups—users and transactions—bipartite graphs excel in depicting interactions without overlap, thus maintaining a clear distinction between participants and their transactions (Geng et al., 2021).

A.1.3 RECURSIVE FEATURE ELIMINATION

After vectorization and feature extraction, we apply recursive feature elimination (RFE) to obtain a compact feature set for the downstream classifiers. RFE iteratively removes the least informative features according to the feedback of the model until a target size is reached. This reduces noise and training cost while preserving the core signal used by the ensemble in the main pipeline (Figure 1).

A.1.4 FEATURE INVENTORY AND DESCRIPTIONS



A

B

Figure 4: Bipartite graph representation of our dataset. Sets A and B demonstrate the accounts and the transactions, respectively. The directed arrows show the sender(s) and receiver(s) of each transaction.

Category	Feature	Brief Description
Graph-Related	in_degree	Number of inbound counterparties (distinct senders).
Graph-Related	out_degree	Number of outbound counterparties (distinct receivers).
Graph-Related	total_degree	Sum of in_degree and out_degree.
Graph-Related	neighbors	Total unique counterparties seen overall.
Graph-Related	in_degree_mean / _max / _min / _median / _std	Statistics of neighbors' inbound degree (structural context).
Graph-Related	out_degree_mean / _max / _min / _median / _std	Statistics of neighbors' outbound degree.
Graph-Related	total_degree_mean / _max / _min / _median / _std	Statistics of neighbors' total degree.
Graph-Related	tx_per_neighbor_mean / _min / _max / _median / _std	Per-neighbor transaction counts aggregated per address.
Graph-Related	multi_transacted_neighbors	Number of counterparties with repeated interactions.
Temporal	n_blocks	Number of distinct blocks in which the address transacted.
Temporal	min_block, max_block	First / last observed block height for the address.
Temporal	block_height_first_sent_in	Block height of the first outgoing transaction.
Temporal	block_height_first_received_in	Block height of the first incoming transaction.
Temporal	block_height_last_sent_in	Block height of the last outgoing transaction.
Temporal	block_height_last_received_in	Block height of the last incoming transaction.
Temporal	transacted_first, transacted_last	First / last timestamp the address was active.
Temporal	Age	Active age (e.g., last minus first activity time).
Temporal	tx_per_block_mean, tx_per_block_max	Average / peak transactions per active block.
Temporal	consistency	Temporal regularity of activity (higher = steadier).
Temporal	burst	Burstiness of activity over time (higher = spikier).
Node	label, tag	Ground-truth / heuristic label or tag if present.
Node	n_tx, n_tx_out, n_tx_in, n_tx_total	Total / outbound / inbound transaction counts.

Continued on next page

Category	Feature	Brief Description
Node	self_tx_count	Number of self-directed transactions (from == to).
Node	n_tokens	Distinct ERC-20 (or other asset) contracts interacted with.
Node	n_method	Distinct method signatures used (diversity of contract calls).
Transaction	n_transfers	Number of native or token transfer events.
Transaction	nERC, n_approve	Count of ERC-20 (etc.) events; number of <code>approve</code> calls.
Transaction	mean_tx_fee / median_tx_fee / max_tx_fee / min_tx_fee / std_tx_fee	Gas-fee statistics over transactions.
Transaction	mean_erc_fee / median_erc_fee / max_erc_fee / min_erc_fee / std_erc_fee	Fee-like statistics derived from token events.
Transaction	mean_out_value_transfer, median_out_value_transfer	Average / median native outgoing amounts.
Transaction	mean_in_value_transfers, median_in_value_transfers	Average / median native incoming amounts.
Transaction	sum_out_value_transfer, sum_in_value_transfer	Total native value outflow / inflow.
Transaction	std_out_value_transfer, std_in_value_transfer	Variability of native transaction amounts.
Transaction	sum_out_value_ERC, sum_in_value_ERC	Total token value outflow / inflow.
Transaction	mean_in_value_ERC, mean_out_value_ERC	Average token amounts incoming / outgoing.
Transaction	median_in_value_ERC, median_out_value_ERC	Median token amounts incoming / outgoing.
Transaction	std_out_value_ERC, std_in_value_ERC	Variability of token transaction amounts.
Volatility	burst, burst_tx_fee, burst_erc_fee	Burstiness in activity and in fee dynamics over time.
Volatility	std_tx_fee, std_erc_fee	Dispersion of fees (higher = more volatile costs).
Volatility	std_out_value_transfer, std_in_value_transfer	Volatility of native transaction amounts.
Volatility	std_out_value_ERC, std_in_value_ERC	Volatility of token transaction amounts.
Volatility	tx_per_block_max	Peak block-level intensity (activity spikes).
Neighborhood	tx_per_neighbor_mean / _min / _max / _median / _std	Stats over per-neighbor transaction counts for the node.
Neighborhood	mean_tx_fee_neighbor_mean / _max / _min / _median / _std	Aggregates of neighbors' mean tx-fees over the neighborhood.
Neighborhood	max_tx_fee_neighbor_mean / _max / _min / _median / _std	Aggregates of neighbors' max tx-fees over the neighborhood.
Neighborhood	mean_erc_fee_neighbor_mean / _max / _min / _median / _std	Aggregates of neighbors' mean ERC fees over the neighborhood.
Neighborhood	max_erc_fee_neighbor_mean / _max / _min / _median / _std	Aggregates of neighbors' max ERC fees over the neighborhood.
Neighborhood	in_degree_mean / _max / _min / _median / _std	Neighbors' inbound-degree statistics (structural context).
Neighborhood	out_degree_mean / _max / _min / _median / _std	Neighbors' outbound-degree statistics.
Neighborhood	total_degree_mean / _max / _min / _median / _std	Neighbors' total-degree statistics.
Neighborhood	multi_transacted_neighbors	Number of counterparties with repeated interactions.

Table 4: Feature inventory by category with brief descriptions.

A.1.5 ISOLATION FOREST SETUP

To handle the large pool of unknown labels, we run Isolation Forest on the unknown subset with a contamination rate of **0.5%**. The predictions partition unknowns into non-outliers (retained as *filtered unknown*) and outliers (treated as *illicit candidates*). We augment the labeled data by adding

the illicit candidates as pseudo-labeled illicit samples. This increases the diversity of illicit examples and helps address class imbalance before supervised training.

To set the Isolation Forest contamination rate, we conducted a small sweep while holding the rest of the pipeline fixed (vectorization, RFE, augmentation protocol, and the confidence level at 0.9). We evaluated three candidates—**0.25%**, **0.5%**, and **1%**—and compared downstream metrics after the increase, focusing on the precision, recall, F1 and overall accuracy of both classes.

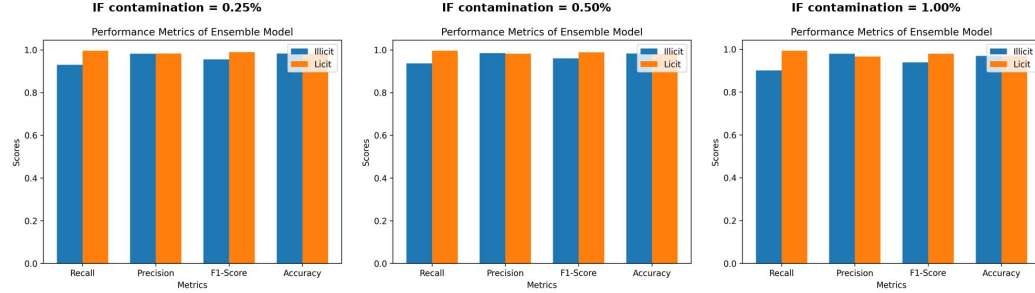


Figure 5: Comparison of Isolation Forest contamination settings (0.25%, 0.5%, 1%) on downstream performance. Panels report precision, recall, F1, and accuracy; 0.5% provides the most consistent balance across metrics.

In practice, while the three contamination settings (0.25%, 0.5%, 1%) yielded broadly similar outcomes (Figure 5), we observed consistent patterns across repeated runs and folds. The 0.25% setting produced a smaller pseudo-labeled set, and 1% offered greater coverage with a modest dip in precision. **We therefore adopt 0.5%**, which stood out across metrics by balancing coverage, precision, and fold-to-fold stability.

A.1.6 MODEL CONFIGURATION, HYPERPARAMETER TUNING, AND CROSS-VALIDATION

The supervised stage combines **Random Forest (RF)** and **XGBoost (XGB)** using *soft voting*. We aggregate *class probabilities* with equal weights, which we found to be stable across folds given the complementary strengths of RF (robustness to heterogeneous features) and XGB (capacity for non-linear interactions).

Random Forest (RF) The objective function defined the hyperparameter search space for the Random Forest model, including parameters such as:

1. **Number of estimators:** The number of trees in the forest.
2. **Maximum of depth:** The maximum depth of each tree.
3. **Minimum samples for splitting:** The minimum number of samples required to split an internal node.
4. **Class weight:** Adjusting the class imbalance.

Each Random Forest model was evaluated using a 5-fold Stratified K-Fold Cross-Validation to ensure that the distribution of illicit and licit labels remained balanced across training and validation splits. Optuna then explored this hyperparameter space and returned the set of parameters that maximized the cross-validated F1-score.

XGBoost (XGB)

Similarly, the objective function defined the hyperparameter search space for the XGBoost model, including:

1. **Maximum depth:** The maximum tree depth.
2. **Learning rate:** The shrinkage factor that controls the step size of updates.

3. **Number of estimators:** The number of boosting rounds.
4. Regularization terms to control overfitting.

As with Random Forest, a 5-fold Stratified Cross-Validation procedure was employed to evaluate model performance. Optuna optimized the hyperparameters by iteratively adjusting them to maximize the F1-score on the validation set.

A.1.7 JUSTIFICATION FOR SELF-LEARNING APPROACH

As observed in the 2D PCA plot (see Figure 6), the data points are widely dispersed across the two principal components. This dispersion indicates that the dataset exhibits substantial variation across different clusters, which aligns with the complex nature of illicit activity patterns in decentralized finance. Given this spread, traditional supervised learning methods may struggle to capture the nuances of each cluster without a sufficiently large labeled dataset.

The SLEID framework’s self-learning approach is particularly suitable in this context, as it leverages unlabeled data through pseudo-labeling. This iterative process enables the model to learn from the underlying structure of the dataset, thus adapting to the dispersed nature of the data without relying solely on labeled samples. The ensemble-based architecture further enhances its ability to generalize across the dispersed clusters, as depicted in the PCA plot, by integrating high-confidence predictions from pseudo-labels in each iteration.

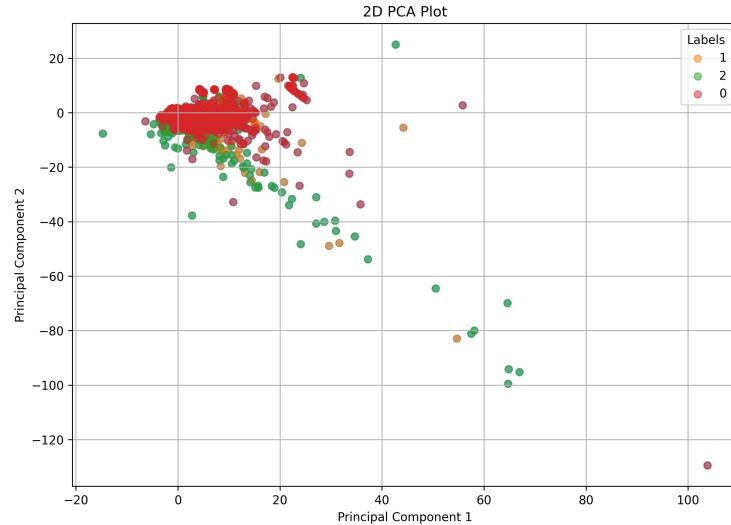


Figure 6: 2D PCA Plot illustrating data dispersion, highlighting the need for a self-learning approach (0 represents unknown accounts, 1 represents illicit accounts, and 2 represents licit accounts.).

A.2 EXPERIMENTS

A.2.1 SELF-LEARNING ITERATION ANALYSIS

Figure 7 illustrates the performance of the illicit class over multiple self-learning iterations. The graph presents metrics such as precision, recall, F1-score, and accuracy across five iterations. Notably, the third iteration yields the best overall performance in terms of illicit precision and F1-score, indicating that additional self-learning iterations do not necessarily lead to performance improvement. After the third iteration, both the F1-score and recall slightly decrease, suggesting diminishing returns from further iterations. The accuracy remains consistently high across all iterations, demonstrating the robustness of the model’s overall performance.



Figure 7: Illicit Class Metrics over Self-Learning Iterations. This figure shows how precision, recall, F1-score, and accuracy fluctuate across five iterations.

A.2.2 MODEL INTERPRETABILITY

To improve the transparency of our SLEID framework, we employed two widely used model-agnostic explanation methods: Local Interpretable Model-agnostic Explanations (LIME) and SHapley Additive exPlanations (SHAP). These tools help us better understand which features drive predictions of illicit activity, thereby addressing one of the limitations of ensemble-based approaches.

LIME (Local Explanation)

Figure 8 illustrates a local explanation for a single account predicted as illicit. The plot shows the top features influencing this decision, with red bars indicating contributions pushing the classification toward the illicit class and green bars indicating contributions toward the licit class. Notably, variables such as number of tokens (n_tokens), number of invoked methods (n_method), and sum of incoming ERC20 value ($sum_in_value_ERC$) play strong roles in shaping the illicit classification. LIME highlights how a relatively small set of features dominates the decision boundary for a given instance, offering actionable insights into why a particular account is flagged.

SHAP (Global Feature Importance)

In contrast, Figure 9 provides a SHAP summary plot capturing feature importance across the entire dataset. The x-axis represents the SHAP value, reflecting the magnitude and direction of each feature's contribution to the model output. Features such as transactions per block ($tx_per_block_mean$, $tx_per_block_max$), degree-related measures (out_degree , $total_degree_min$, out_degree_median), and transaction fee statistics ($max_tx_fee_mean$, $mean_tx_fee_max$) are identified as globally important. The color scale indicates feature values (red = high, blue = low), helping interpret how high or low values affect predictions. For instance, accounts with high $tx_per_block_mean$ values are more likely to be classified as illicit.

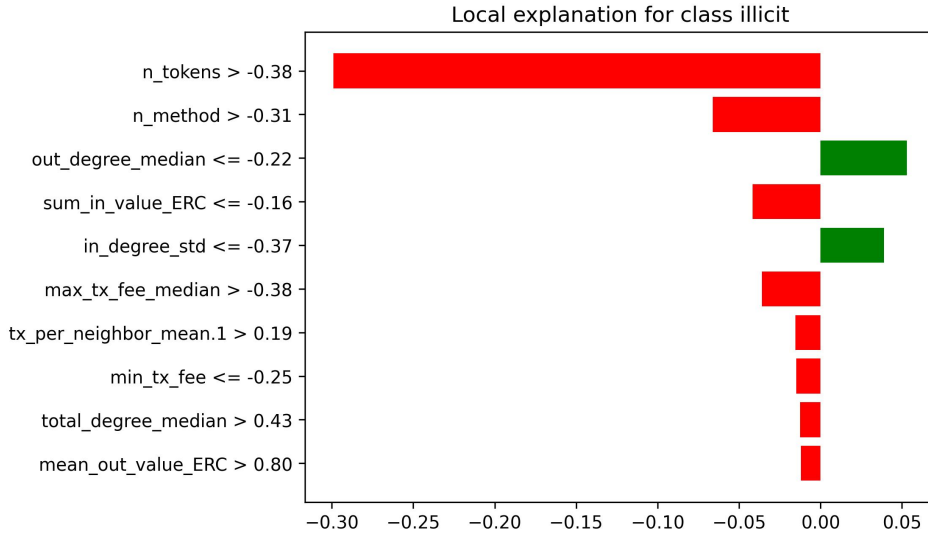


Figure 8: Local LIME explanation for a single account predicted as illicit. Red bars push toward the illicit class and green bars toward the licit class; features such as n_tokens , n_method , and $sum_in_value_ERC$ drive the decision.

Together, LIME and SHAP provide complementary interpretability:

- LIME offers local, instance-specific explanations, showing why an individual account is considered suspicious.
- SHAP provides a global view of feature importance, highlighting which features consistently influence predictions across the dataset.

By incorporating these explainability techniques, we improve the trustworthiness of our framework and provide regulators and practitioners with interpretable insights into how illicit activity is detected on the Ethereum blockchain.

A.2.3 FEATURE IMPORTANCE ANALYSIS

To further examine the drivers of our model’s predictions, we analyze the feature importance scores, as illustrated in Figure 10. The results reveal that transaction-related variables dominate the model’s decision-making process. In particular, $tx_per_block_max$ and $tx_per_block_mean$ emerge as the most influential features, suggesting that accounts with consistently high or spiked transaction activity per block are strongly associated with illicit behavior. Transaction fee statistics, such as max_tx_fee , also play a significant role, highlighting how unusually large fees may indicate suspicious activity. Additionally, degree-related measures, including out_degree_min , $total_degree_min$, and out_degree , demonstrate the importance of network connectivity patterns in distinguishing between licit and illicit accounts. Secondary features, such as out_degree_mean , $max_tx_fee_median$, and $mean_tx_fee$, contribute to refining the model’s sensitivity to subtle behavioral signals. Together, these findings confirm that both transaction intensity and structural network characteristics are critical factors for detecting illicit activity on the Ethereum blockchain.

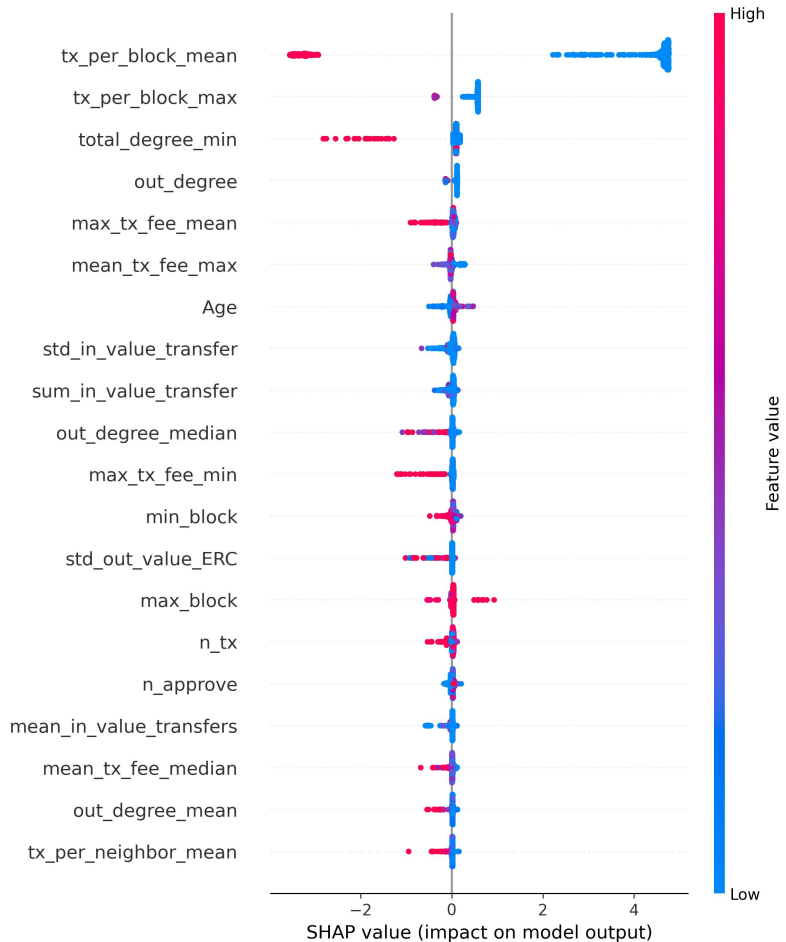


Figure 9: SHAP summary plot showing global feature importance across the dataset. Transaction intensity ($tx_per_block_mean$, $tx_per_block_max$), degree measures (out_degree , $total_degree_min$, out_degree_median), and fee statistics ($max_tx_fee_mean$, $mean_tx_fee_max$) dominate; color encodes feature value (red = high, blue = low).

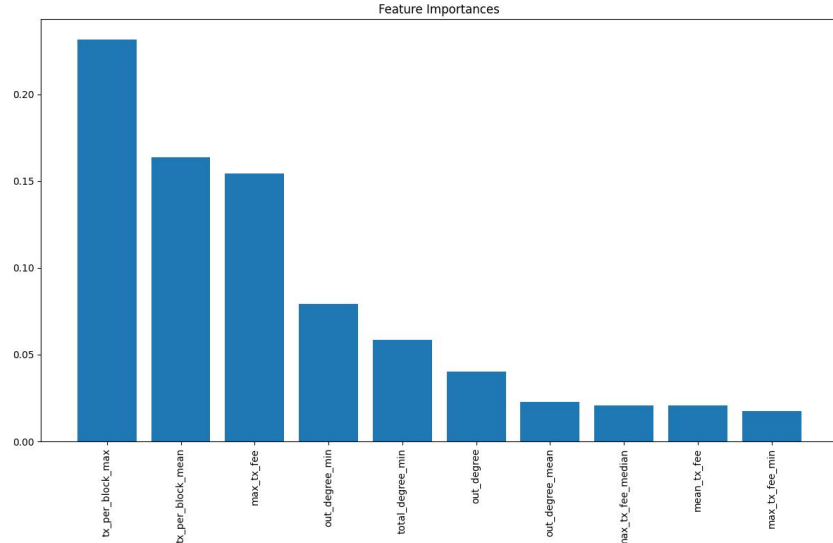


Figure 10: XGBoost feature importance showing that transaction intensity, fee patterns, and network connectivity are most influential in distinguishing illicit from licit accounts.

A.2.4 FALSE POSITIVES ANALYSIS

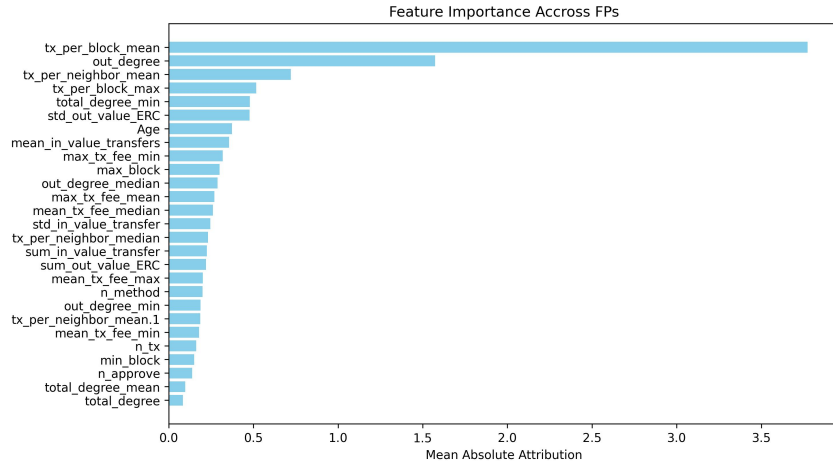


Figure 11: Feature attributions for top false positives. Elevated activity and connectivity characteristics push illicit probabilities above 0.9 for licit accounts, indicating over-sensitivity to high-volume behavioral patterns.

The analysis of the top false positives reveals that the model often misclassifies licit accounts with unusually high transaction activity and degree-related measures, leading to predicted probabilities above 0.9 despite their true non-illicit label. Across these cases, features such as *tx_per_block_mean*, *tx_per_block_max*, and *out_degree* frequently appear among the top SHAP attributions, indicating that intense transaction patterns and broad connectivity strongly bias the model toward the illicit class. This suggests that while the classifier is highly sensitive to behaviors resembling illicit accounts, it can overgeneralize when legitimate accounts exhibit similar structural or transactional intensity. These findings highlight the need to refine thresholds, incorporate additional contextual features (e.g., temporal behavior, account type), or calibrate the model to reduce costly false positives without undermining illicit detection sensitivity.

A.2.5 EVALUATION UNDER CLASS IMBALANCE

Illicit accounts are rare and false positives are costly; accuracy/ROC can be misleading in this regime. We therefore report imbalance-aware metrics and briefly assess FP risk.

We use (i) *PR-AUC on the minority class* to judge ranking quality when positives are scarce, (ii) *class-weighted F1* to balance precision/recall under skew, and (iii) *MCC* as a single, balanced correlation of the confusion matrix.

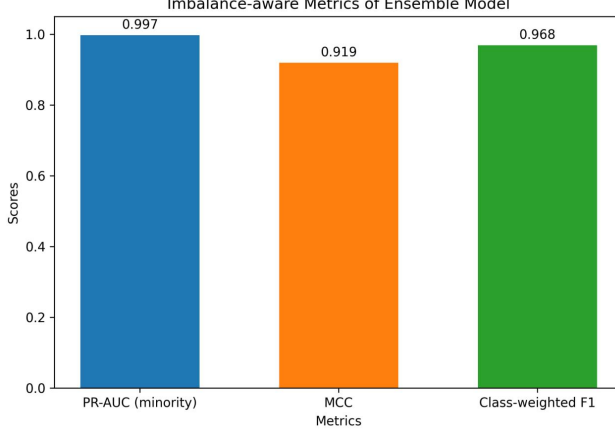


Figure 12: Imbalance-aware metrics for SLEID: PR-AUC (minority), MCC, and class-weighted F1.

As shown in Fig. 12, SLEID attains **PR-AUC** ≈ 0.997 , **MCC** ≈ 0.919 , and **class-weighted F1** ≈ 0.968 . These indicate (a) near-perfect ranking of illicit vs. benign accounts, (b) balanced errors rather than majority-class bias, and (c) strong precision–recall trade-offs at class-aware operating points.